

**Report No.
CVEEN-02/02**

**FATIGUE TESTS OF CRACKED AND
REPAIRED ALUMINUM CONNECTIONS
OF OVERHEAD SIGN STRUCTURES –
INTERIM REPORT**

by

CHRIS P. PANTELIDES

JUSTIN NADAULD

Report to Sponsors:

**New York State Department of Transportation
Utah Department of Transportation**

June 2002

**Civil & Environmental Engineering
College of Engineering
University of Utah
Salt Lake City, Utah**

Report No. CVEEN-02/02

**FATIGUE TESTS OF CRACKED AND REPAIRED ALUMINUM
CONNECTIONS OF OVERHEAD SIGN STRUCTURES -
INTERIM REPORT**

by

CHRIS P. PANTELIDES¹

JUSTIN NADAULD²

¹Professor of Civil & Environmental Engineering

²Research Assistant

Report to Sponsors:

**New York State Department of Transportation
Utah Department of Transportation**

**Civil & Environmental Engineering
College of Engineering
University of Utah
122 South Central Campus Drive Rm 104
Salt Lake City UT 84112-0561**

June 2002

FORWARD

University of Utah Professor Chris P. Pantelides obtained a research grant from the New York State Department of Transportation (NYSDOT) and the Utah Department of Transportation (UDOT) for performing a research study regarding the fatigue evaluation of aluminum connections, both cracked and uncracked, of overhead sign structures. In addition, the fatigue evaluation of repaired aluminum connections with glass fiber reinforced polymer composites was performed.

Principal investigator for the project was Professor Chris P. Pantelides, and co-principal investigator was Professor Lawrence D. Reaveley of the Department of Civil and Environmental Engineering. Justin Nadauld, graduate student at the Civil and Environmental Engineering Department, and Oliver Burt, undergraduate student at the Civil and Environmental Engineering Department, were the research assistants for the project.

This document constitutes the Interim Report for the project. The NYSDOT manager for the project was Harry White, P.E., and the UDOT manager for the project was Doug Anderson, P.E.

ACKNOWLEDGEMENTS

The authors would like to thank the following individuals for their support and encouragement throughout the project: Harry White of NYSDOT; Doug Anderson and Samuel Musser of UDOT; and Dr. Larry Cercone, Franz Worth, and Steve Bazinet of Air Logistics Corporation.

In addition, the authors would like to thank Chris Delahunty, M.Sc., and Oliver Burt, B.Sc., from the Civil and Environmental Department, University of Utah.

Finally, the authors would like to thank Air Logistics Corporation for the in-kind support and their technical expertise.

TABLE OF CONTENTS

FORWARD.....	iii
ACKNOWLEDGEMENTS.....	iv
LIST OF FIGURES	vi
LIST OF TABLES.....	vii
1. Introduction.....	1
2. Objectives	2
3. Technique.....	3
Series (I): Static Tests	3
Series (II): Fatigue Tests of As-is Welded Aluminum Connections with No Visible Cracks...	5
Series (III): Fatigue Tests of Cracked Aluminum Connections from the Field Repaired with GFRP.....	8
Series (IV): Fatigue Tests of Tack-welded Aluminum Connections Retrofitted with GFRP.....	8
4. Experimental Results	9
5. Observations and Preliminary Conclusions	19
6. References.....	20

LIST OF FIGURES

Fig. 1.	Tri-truss aluminum overhead sign support structure.....	1
Fig. 2.	Crack through aluminum-welded joint of overhead sign structure	1
Fig. 3.	Test Setup for Static and Fatigue Tests	4
Fig. 4.	Constant Amplitude Fatigue Test.....	7
Fig. 5.	Test I-a: (a) Failure of Diagonal, (b) Failure of chord at toe of weld.....	10
Fig. 6.	Test I-a Load vs. Displacement curve	10
Fig. 7.	Test II-b: Fatigue test of as-is welded joint: (a), and (b) Typical failure of series II tests.....	11
Fig. 8.	Typical displacement of series II tests, test II-b is shown	11
Fig. 9.	Test III-a: (a), and (b) Failure of weld and FRP composite	12
Fig. 10.	Displacement vs. Cycles curve for test III-a.....	12
Fig. 11.	Test III-a: (a), and (b) Failure of weld and FRP composite	13
Fig. 12.	Displacement vs. Cycles curve for test III-b	13
Fig. 13.	(a) Crack in FRP after 1×10^6 cycles, (b) Picture of III-c after static test to failure	14
Fig. 14.	Static test of test III-c after 1×10^6 cycles.....	14
Fig. 15.	Adhesive failure of test IV-c	15
Fig. 16.	Displacement vs. Cycles curve for test IV-b	15
Fig. 17.	S-N Curves	18

LIST OF TABLES

Table 1.	Constant-Amplitude Fatigue Threshold.....	6
Table 2.	Test Matrix for Fatigue Tests of As-is Welded Aluminum Connections With no Visible Cracks.....	7
Table 3.	Test Matrix for Fatigue Tests of Cracked Aluminum Connections From the Field Repaired With GFRP	8
Table 4.	Test Matrix for Fatigue Tests of Tack-welded Aluminum Connections Retrofitted With GFRP.....	8
Table 5.	Aluminum Tube Dimensions.....	9
Table 6.	Summary of Experimental Results.....	17

1. Introduction

Cracks in the welds of aluminum overhead sign structures can propagate to complete failure of members, which can cause signs to fall and cause injuries. The truss considered here is a 3D truss, or tri-truss system, as shown in Fig. 1. Figure 2 shows a typical crack in a welded aluminum connection, which typically occurs due to thermal and fatigue stresses.



Fig. 1. Tri-truss aluminum overhead sign support structure



Fig. 2. Crack through aluminum-welded joint of overhead sign structure

A repair method for cracked aluminum welded connections of overhead sign structures using glass fiber reinforced polymer GFRP composites had been investigated previously (Pantelides and Nadauld 2001). The tests performed in that investigation consisted of pulling the diagonal members from the joint with the chord member in monotonic static tension. The as-is aluminum welded connection without any visible cracks was able to resist a stress of 14.0 ksi or 1.16 times the allowable stress for welded tubes according to the *Aluminum Association Specifications* (1986). The GFRP composite repaired field connections with cracks in the welds, which ranged from $\frac{1}{4}$ to $\frac{2}{3}$ of the total weld length, reached static monotonic tensile stress capacities of 16.4 ksi to 17.45 ksi, which constitutes a ratio of 1.17 to 1.25 times that of the as-is welded connection with no visible cracks. The experimental results of that study had demonstrated that the method developed was a viable repair technique for cracked welded connections of aluminum sign structures.

The tests performed in the recently completed investigation were static tension tests; the current research targets the fatigue life of the as-is connections without any visible cracks, and that of the repaired connections with GFRP composites. This is important for determining how many cycles to failure the repaired connection with GFRP composites can tolerate. The tests carried out in this research also provide fatigue information about the as-is welded connections, which were obtained from the field in two conditions: (a) cracked condition, (b) uncracked condition. The uncracked connections were tested to determine the fatigue life of the as-is aluminum connections in the field. The cracked connections were also obtained from the field; they were repaired with GFRP composites and then subjected to identical fatigue tests as the uncracked aluminum connections. In addition, new aluminum connections were fabricated by tack-welding the aluminum tubes at only four points to form the geometry, then wrapping the joints to form an all-composite GFRP connection. These connections form the third series of fatigue tests. This interim report provides comparisons between the number of cycles to failure of the as-is uncracked specimens and the repaired specimens with GFRP composites; it is believed that these comparisons can provide engineers useful information about the expected life of the repaired connections.

2. Objectives

The overall objective of the present study is to investigate the performance of the as-is and repaired aluminum connections with GFRP composites under fatigue loads. The aluminum connections were subjected to constant amplitude fatigue tests at three stress ranges and at a fixed frequency of 2 Hz. The ultimate goal is to determine the strength of the as-is and repaired connection after it has withstood fatigue loading at various stress ranges up to 1,000,000 cycles and the remaining static load capacity after this number of cycles if the connection reaches 1,000,000 cycles. In addition to the fatigue tests, two additional static tests for uncracked aluminum joints from the field were performed to establish the static load capacity of the as-is joints.

3. Technique

NYSDOT has provided twelve (12) field collected truss sections for performing the fatigue tests with dimensions shown in Table 5; of these, six (6) were uncracked sections and six (6) cracked sections. Two (2) of the six uncracked sections were provided by NYSDOT to perform two static tension tests following the procedures described in the completed investigation (Pantelides and Nadauld 2001). Seven (7) tack-welded aluminum specimens were provided by Air Logistics Corporation for a series of fatigue tests on GFRP retrofitted specimens; these specimens demonstrate the fatigue strength of the connection with only the GFRP composite contribution. This series is expected to produce the true strength of the GFRP connection after fatigue loading at various stress ranges, since there will be no strength offered by the aluminum weld.

Two types of tests were performed: static and fatigue tests as described below. The static tests were for two aluminum truss specimens from the field, and constitute tensile tests to failure (Series I). The fatigue tests were of three types: (Series II) as-is aluminum truss specimens from the field with no visible cracks, (Series III) cracked aluminum truss specimens from the field repaired with GFRP, and (Series IV) tack-welded aluminum specimens retrofitted with GFRP.

Series (I): Static Tests

Two (2) tests of uncracked specimens to failure were performed. One test had already been performed in a previous study (Pantelides and Nadauld 2001) and the two additional tests were performed in order to assist in the determination of the average static tension capacity of the uncracked joints using the three test results. However, the failure modes and geometry of the two new tests were different from those of the first test; see Table 5 and Chapter 4 on failure modes. Therefore only the two recent tests were used to determine the average static tension capacity of uncracked joints. The tests were performed in the existing fixture as shown in Fig. 3.

The results of the two static tests were as follows:

Test I(a): Tensile failure load = 28.8 kips (128.1 kN)

Test I(b): Tensile failure load = 28.3 kips (125.9 kN)

The average static tensile load carried by the uncracked aluminum joint is evaluated as 28.6 kips (127.2) kN.

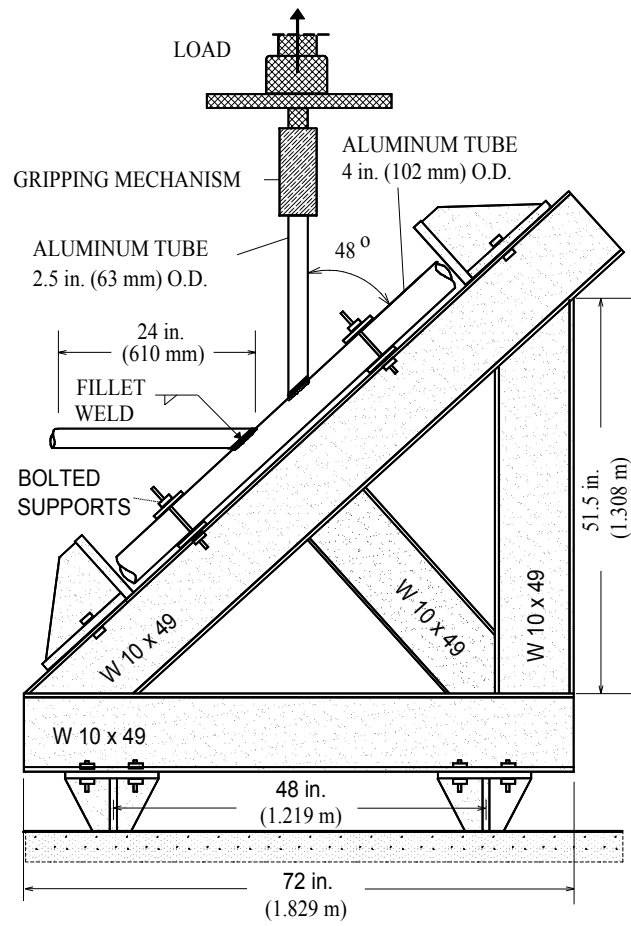


Fig. 3. Test Setup for Static and Fatigue Tests

Series (II): Fatigue Tests of As-is Welded Aluminum Connections with No Visible Cracks

Fatigue failure of aluminum overhead sign structures may occur during fabrication, transportation to the site, erection, and operation or service. Several examples exist of fatigue failures not caused by operating loads but rather by cyclic loads that occurred during their shipment to the site. A large percentage of fatigue cracks are caused by wind-induced vibration of members that are too slender (Sharp et al. 1996). Repairing of welded aluminum connections in the field is generally not recommended because of the difficulty in maintaining the gas enclosure over the arc in the wind. For repair of cracks in groove-welded plate specimens using welds, it has been noted that even though good practice was employed in making the repairs, the geometry of the bead, the quality of the weld, and the fatigue life were generally not as good as those of the original joint (Sharp et al. 1996).

Fatigue data on failure of welded joints in tubular aluminum trusses show that such failures can be calculated using the total applied stress at the edge of the weld, that is, the axial and bending stress in the member added to the stress from local bending of the tube wall. To obtain these stresses, a finite element analysis of the truss must be made. The fatigue failure in tests for welded joints in tubular aluminum trusses occurred in the range of 10,000 to 2 million cycles, depending on the level of maximum stress range (Sharp 1993).

The 1975 edition of the *Standard Specifications for Structural Supports for Highway Signs, Luminaires and Traffic Signals* (AASHTO 1975) suggests that sound practice in designing highway signs should be based on the infinite life (endurance limit) of the materials. This generally represented the 2 million-cycle failure stress for steel, and the 500-million-cycle failure stress for aluminum. However, it should be noted that these figures represent welds of new structures without fatigue cracks. In the 1996 AASHTO *Standard Specifications*, the constant amplitude fatigue threshold was termed the allowable fatigue stress range for more than 2 million cycles on a redundant load path structure (AASHTO 1998). The fourth edition of the *Standard Specifications for Structural Supports for Highway Signs, Luminaires and Traffic Signals* (AASHTO 2001) adopts an infinite life design approach for fatigue design criteria. This is considered sound practice and is generally based on the Constant Amplitude Fatigue Limit (CAFL) as shown in Table 1.

Table 1. Constant-Amplitude Fatigue Threshold

Detail Category	Aluminum Threshold (ksi)
A	10.2
B	6.0
B'	4.6
C	4.0
D	2.5
E	1.9
E'	1.0
ET	0.44
K ₂	0.38

Details provided in the fourth edition of the *Standard Specifications for Structural Supports for Highway Signs, Luminaires and Traffic Signals* (AASHTO 2001) classify the joint under investigation as Detail 19 (Example 10) fillet welded T-, Y-, and K-tube-to-tube connection for which the stress category with respect to stress in the chord is Category E. Using an area of 1.767 in² for the diagonal brace member gives an applied load of 3.4 kips for the load corresponding to the CAFL threshold.

The University of Utah has a 220 kip programmable MTS actuator, which was used to test the joint specimens in fatigue. The actuator has been used to perform such studies in the past, namely the fatigue strength of carbon FRP retrofitted concrete bridge decks with corroded rebar. The present tests were performed in the same fixture as shown in Fig. 3. From measurements of vibration on actual aluminum highway sign structures, the range of frequencies of such structures ranges from 0 to 5 Hz. The frequency of the fatigue cycles used in the present tests was 2 Hz, i.e., two cycles per second. The definition of the terms maximum stress, minimum stress, mean stress, stress range, and stress ratio is also given in Fig. 4.

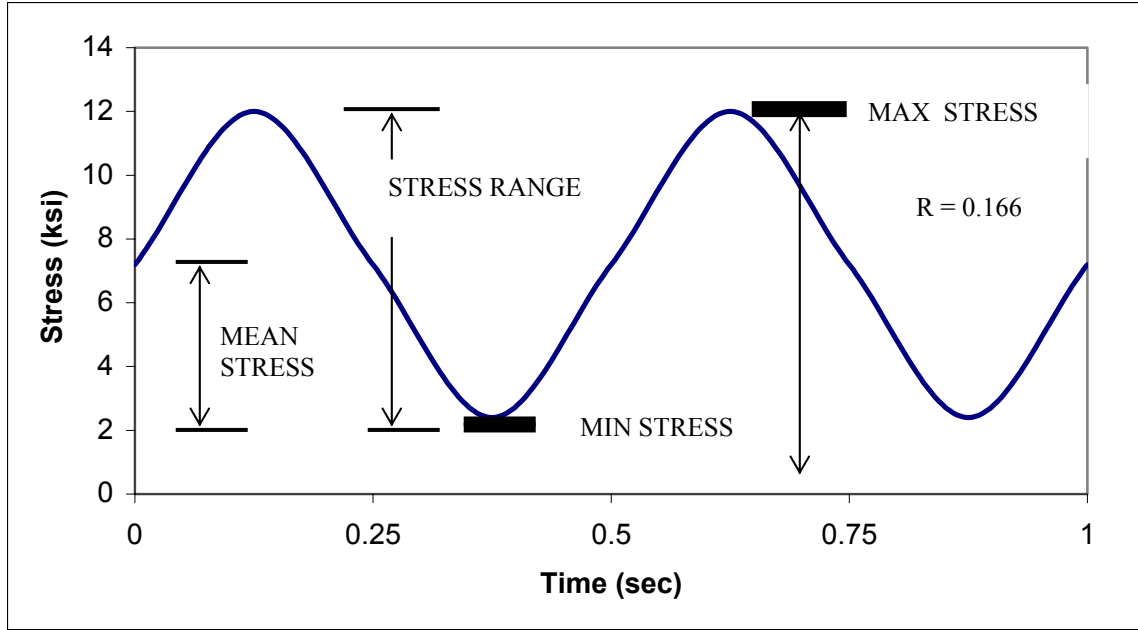


Fig. 4. Constant Amplitude Fatigue Test

It should be noted that the minimum stress that will be used in the tests is higher than zero, as shown in Fig. 4. The stress ratio $R = (\text{min. stress} / \text{max. stress})$ used in the tests was close to $R = 0.20$. (In Fig. 4 $R = 2/12 = 0.166$).

In the present tests, the maximum number of cycles was limited to 1 million, followed by a static test if the joint survives the 1,000,000 cycles. The maximum number of cycles is significant, since 1,000,000 cycles is equivalent to 100 cycles per day, every day for approximately 27.4 years. It should also be noted that the 1,000,000 cycle series at 2 Hz frequency takes approximately 6 days continuously to be completed. The static test following the 1,000,000 fatigue cycles represents the remaining life of the joint.

Given the above information, the test series shown in Table 2 was used for fatigue testing of as-is welded aluminum connections with no visible cracks.

Table 2. Test Matrix for Fatigue Tests of As-is Welded Aluminum Connections With No Visible Cracks

<i>Specimen</i>	<i>Condition</i>	<i>Source</i>	<i>Test</i>	<i>Stress (ksi)</i>
II-a	Uncracked	NYSDOT	Cycle to failure at 21 kips	12.0
II-b	Uncracked	NYSDOT	Cycle to failure at 15 kips	8.5
II-c	Uncracked	NYSDOT	Cycle to failure at 10 kips	5.7

In Table 2, the upper stress level is 21 kips, which corresponds to a stress of 12 ksi that is the static design, and is 85% of the strength of a static test performed in the earlier study (Pantelides and Nadauld 2001), and 73% of the test Series (I) results carried out in the present study. Note also that this stress is higher than the Detail Category A stress of Table 1

recommended in AASHTO (2001), by a factor of 1.17; in addition, a fourth test will be carried out in a later phase of the current experimental program at a stress of 3.4 ksi, which is 1.79 times the Constant-Amplitude Fatigue Threshold of Table 1 for Detail Category E. However, it should be noted that Table 1 refers to design criteria, which are conservative, as opposed to Table 2, which draws upon the experience from actual test results. It is believed that the four stress levels of 3.4 ksi, 5.7 ksi, 8.5 ksi and 12 ksi provide a large enough spread so that a good distribution of stress range versus number of cycles to failure can be obtained.

Series (III): Fatigue Tests of Cracked Aluminum Connections from the Field Repaired with GFRP

The test series shown in Table 3 was used for fatigue testing of cracked aluminum connections from the field repaired with GFRP.

Table 3. Test Matrix for Fatigue Tests of Cracked Aluminum Connections From the Field Repaired With GFRP

<i>Specimen</i>	<i>Condition</i>	<i>Source</i>	<i>Test</i>	<i>Stress (ksi)</i>
III-a	Cracked/GFRP wrapped	NYSDOT	Cycle to failure at 21 kips	12.0
III-b	Cracked/GFRP wrapped	NYSDOT	Cycle to failure at 15 kips	8.5
III-c	Cracked/GFRP wrapped	NYSDOT	Cycle to failure at 10 kips	5.7

In Table 3, the upper stress level is 21 kips, which corresponds to a stress of 12 ksi. This is the same as that of the as-is uncracked specimens of Test Series (II). The same strategy will be used as for Test Series (II) regarding the remaining three specimens.

Series (IV): Fatigue Tests of Tack-welded Aluminum Connections Retrofitted with GFRP

The test series shown in Table 4 was used for fatigue testing of tack-welded aluminum connections repaired with GFRP. This series is expected to produce the true strength of the GFRP connection after fatigue loading at various stress ranges, since there will be no strength offered by the weld. The same strategy will be used as for Test Series (II) regarding the remaining three specimens.

Table 4. Test Matrix for Fatigue Tests of Tack-welded Aluminum Connections Retrofitted With GFRP

<i>Specimen</i>	<i>Condition</i>	<i>Source</i>	<i>Test</i>	<i>Stress (ksi)</i>
III-a	GFRP wrapped	Air Logistics	Cycle to failure at 21 kips	12.0
III-b	GFRP wrapped	Air Logistics	Cycle to failure at 15 kips	8.5
III-c	GFRP wrapped	Air Logistics	Cycle to failure at 10 kips	5.7

4. Experimental Results

This chapter describes the experimental results obtained in both the static and fatigue load tests carried out up to June 2002. The test units used in this study had various dimensions and thickness as shown in Table 5. The geometry of all of the test units was the same in all tests.

Table 5. Aluminum Tube Dimensions

	Pipe (1)	O.D. mm (in) (2)	I.D. mm (in) (3)	Thickness mm (in) (4)	Area mm ² (in ²) (5)
TYPE I	Diagonal Braces	63.5 (2 ½)	50.8 (2)	6.35 (¼)	1,140 (1.767)
	Main Chord	101.6 (4)	88.9 (3 ½)	6.35 (¼)	1,900 (2.945)
TYPE II	Diagonal Braces	63.5 (2 ½)	53.9 (2.125)	4.76 (3/16)	878.8 (1.362)
	Main Chord	101.6 (4)	88.9 (3 ½)	6.35 (¼)	1,900 (2.945)

The two types of aluminum tube dimensions were used in a random manner, based on the limited number of test units available. However, in the summary of results the individual units are identified as either Type I or Type II.

In what follows the failure modes observed in the four different test series are identified and described using experimental data and photographic documentation.

Series (I) Results

Static tests I-a and I-b had a similar failure mode and load/displacement curve. Failure occurred at the toe of the weld and continued almost entirely around the chord, as can be seen in Fig. 5. Immediately following failure of the chord the diagonal was subjected to combined tensile and bending stress, due to the large deflection of the chord, which subsequently caused the diagonal to fail as seen in Fig. 6. This failure of the diagonal was secondary to the failure of the chord.

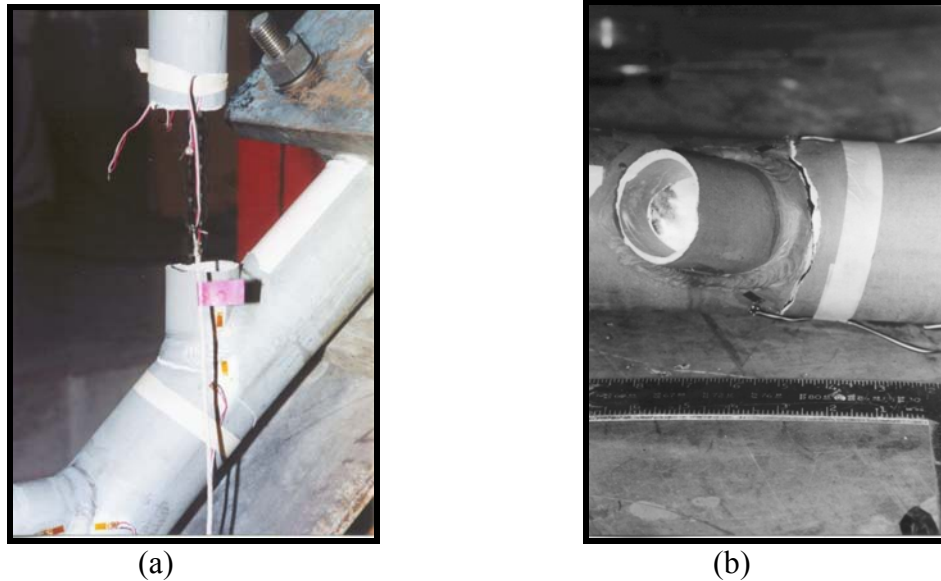


Fig. 5. Test I-a: (a) Failure of Diagonal, (b) Failure of chord at toe of weld

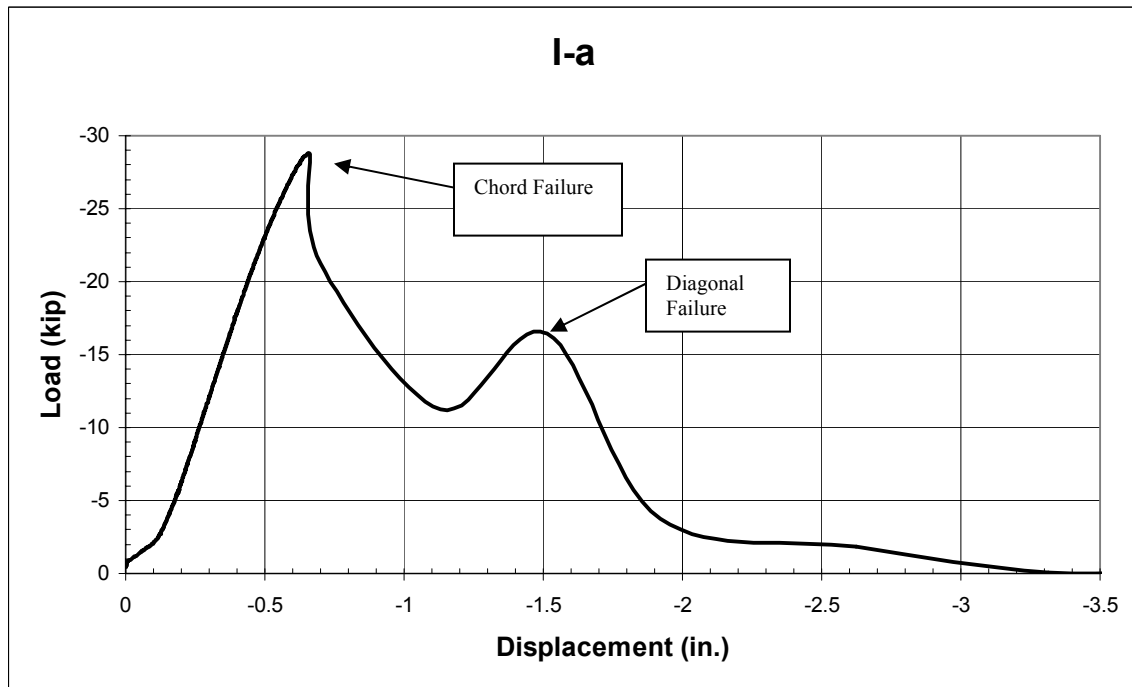
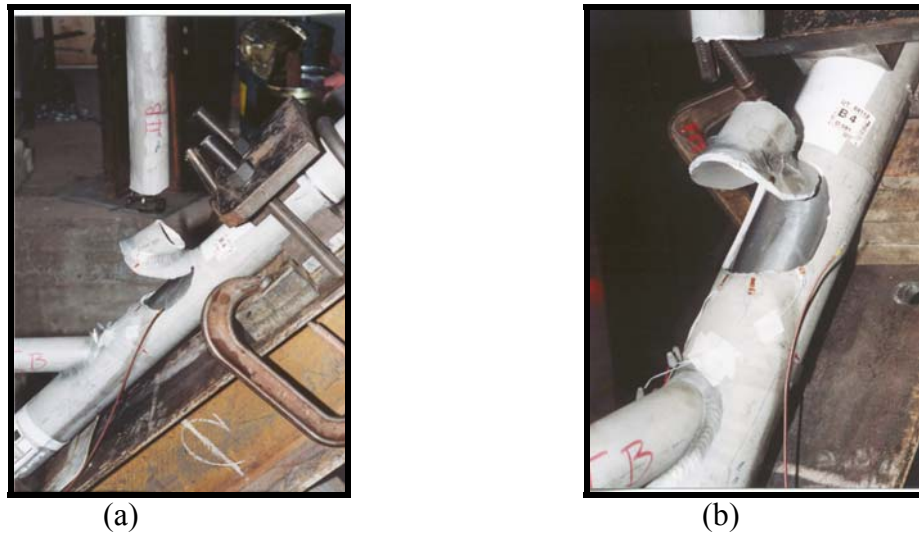


Fig. 6. Test I-a Load vs. Displacement curve

Series (II) Results

Series (II) tests all had a similar failure mode and displacement/cycle curve. The typical failure is seen in Figs.7 and 8. The failure started with a crack at the toe of the weld; the crack propagated into the base material, and would have continued around the chord – similar to the failure of the series I tests. However, the steel pipe inside the chord forced the crack to propagate through the base material outside the weld, a distance of $\frac{1}{2}$ " to 1" following the weld contour, as shown in Fig. 7(b). Figure 8 shows the typical displacement vs. number of cycles curve for the Series (II) tests. The top line shows the displacement at the maximum stress (0.22in.) and the bottom line shows the displacement at the minimum stress (0.13in.). At approximately 31,000 cycles the displacements start to increase indicating gradual degradation to failure.



**Fig. 7. Test II-b: Fatigue test of as-is welded joint; (a), and (b)
Typical failure of series II tests**

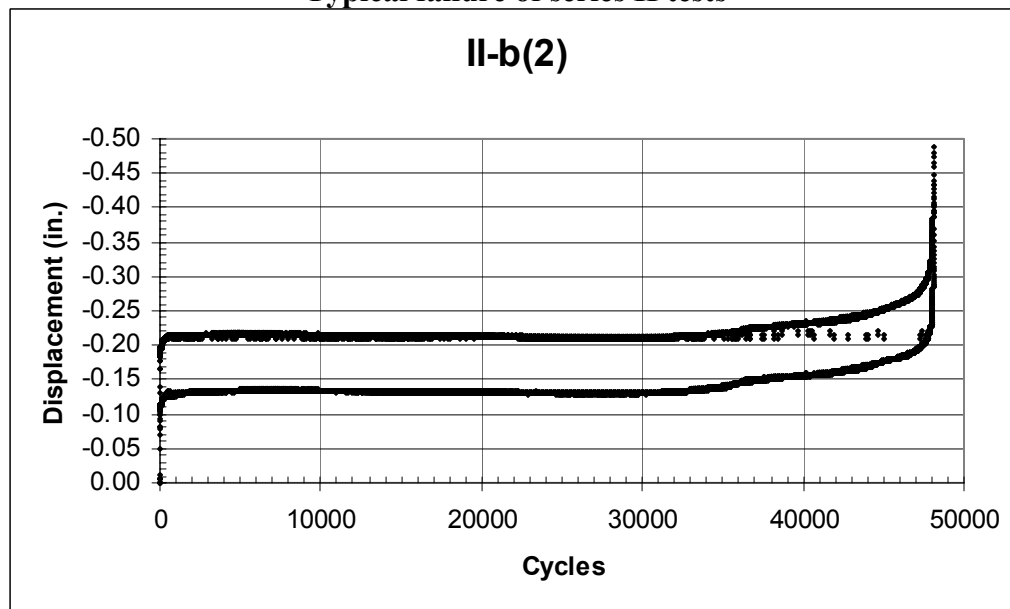


Fig. 8. Typical displacement of series II tests, test II-b is shown

Series (III) Results

Failure Mode 1: Weld Throat Cracking and FRP Failure

Series (III) tests had two basic failure modes. The first is shown in Fig. 9 and Fig. 10. This failure consisted of initial cracking of the FRP composite (note the horizontal lines in Fig. 9) followed by cracking failure through the throat of the weld and finally by tensile failure of the FRP composite. It can be seen in Fig. 10 that the weld failed at about 5000 cycles, and the FRP composite failed much later at 6763 cycles.

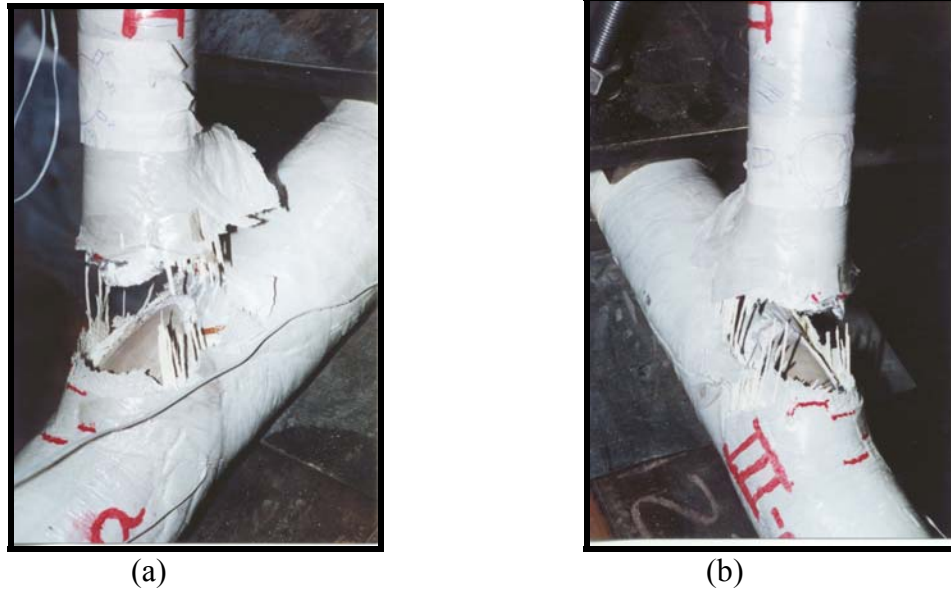


Fig. 9. Test III-a: (a), and (b) Failure of weld and FRP composite

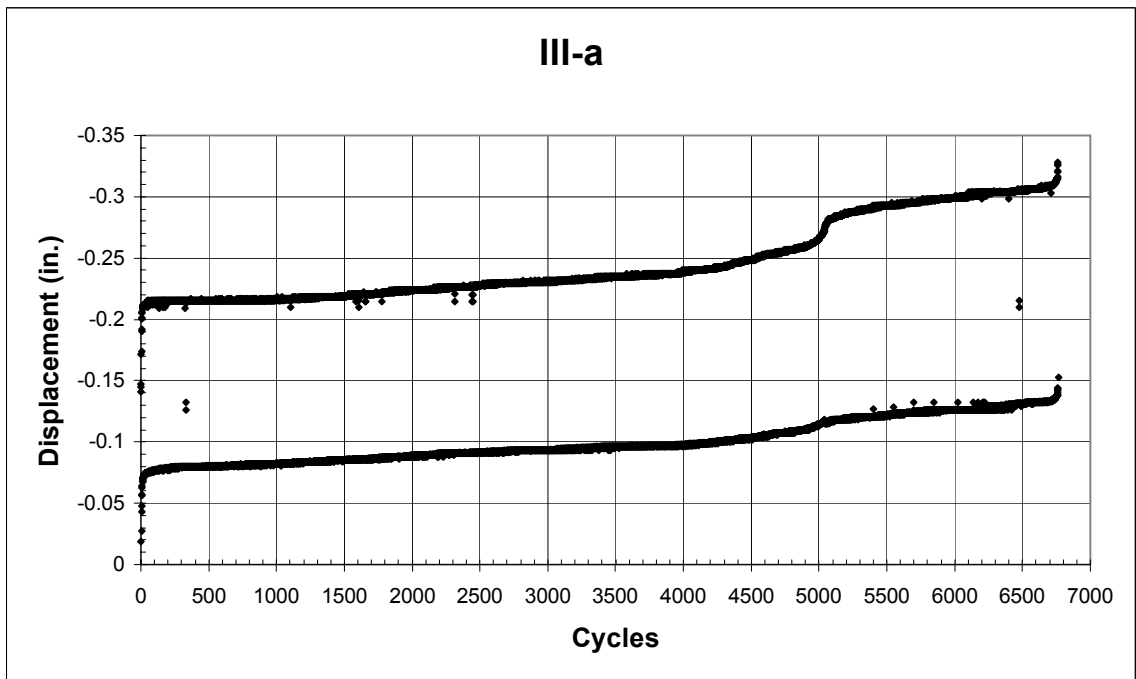


Fig. 10. Displacement vs. Cycles curve for test III-a

Failure Mode 2: Toe Weld Cracking followed by Throat Weld Cracking and FRP Failure

The second failure mode seen in the Series (III) tests is shown in Fig. 11 and Fig. 12. This failure was seen in tests III-b and III-c. In this failure mode cracking was seen on the FRP first. This cracking was directly above the initial crack of the aluminum induced during the test at the toe of the weld; this failure was not through the throat of the weld. This crack at the toe of the weld propagated around the chord, similar to the failure mode of Series (II) tests. As can be seen in Fig. 12, this occurred between 8,000 and 12,000 cycles. Next the weld was slowly fatigued, this occurred in the throat of the weld, until the weld completely fractured. This was followed by tensile failure of the FRP composite.



Fig. 11. (a) Initial cracking of FRP composite, (b) Failure of Base Material, Weld, and FRP composite

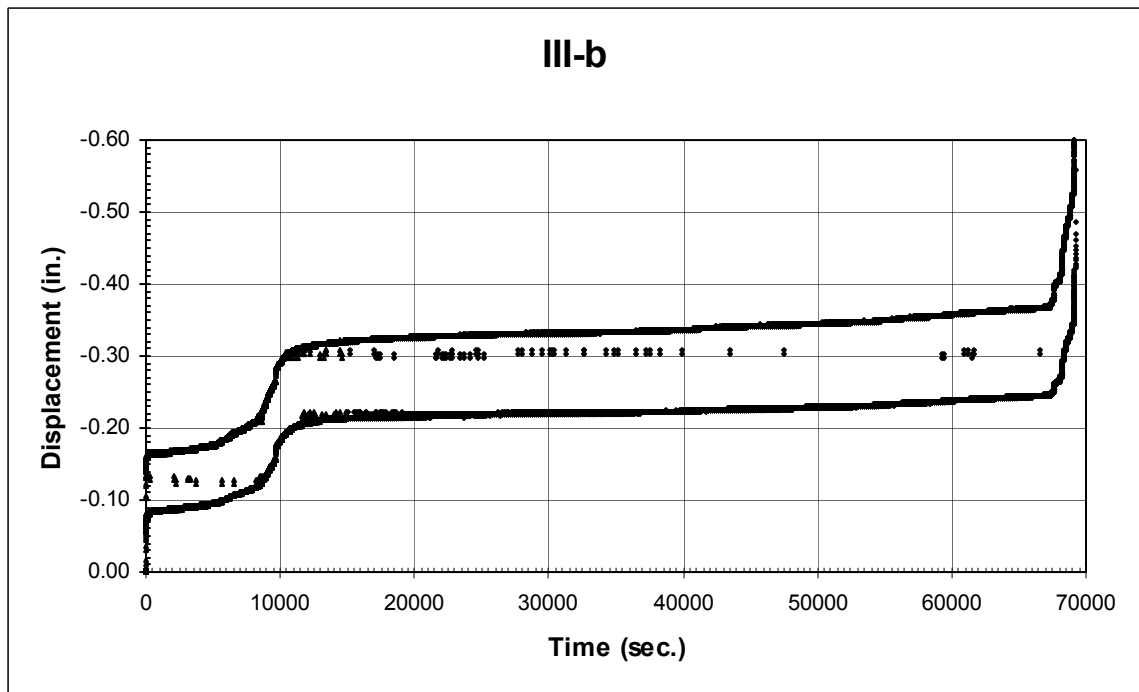


Fig. 12. Displacement vs. Cycles curve for test III-b

Test III-c was fatigued until 1,000,000 cycles were reached. After 1×10^6 cycles the crack in Fig. 13(a) had formed. The remaining strength of the connection after 1×10^6 cycles was determined with a tensile static test, as in test Series (I). The static test revealed a failure mode similar to test III-b, i.e. Failure Mode 2, which included failure of the aluminum at the toe of the weld, followed by failure of the weld through the throat of the weld, and finally failure of the FRP composite. This progressive failure can be seen in the load/ displacement graph in Fig. 14.

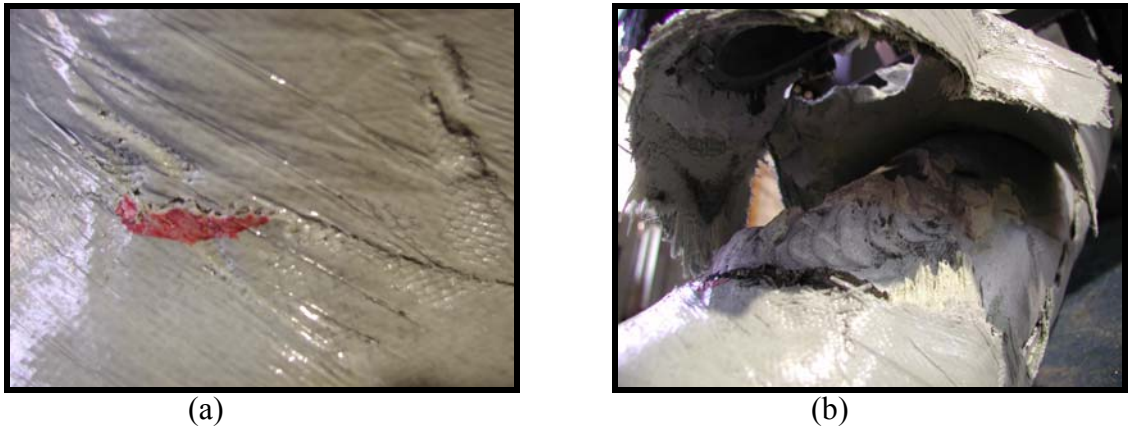


Fig. 13. (a) Crack in FRP after 1×10^6 cycles, (b) Picture of III-c after static test to failure

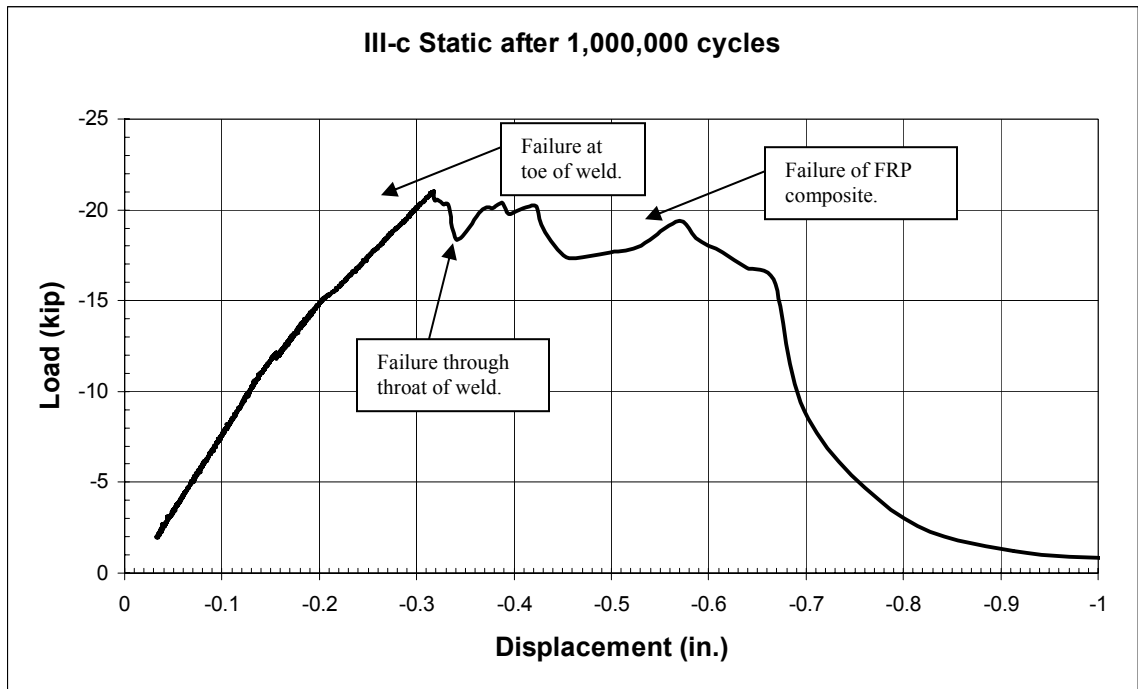


Fig. 14. Static test of test III-c after 1×10^6 cycles

Series (IV) Results

Series (IV) tests had two failure modes, adhesive and FRP composite tensile failure. The adhesive failure occurred in tests IV-a (1) and IV-c. The adhesive failure of test IV-c is shown in Fig. 15. This failure is identical to the adhesive failure described in a previous report regarding static tests of similar joints (Pantelides and Nadauld 2001). Test IV-a was repeated to determine if the adhesive failure was due to quality control issues. This second test, IV-a (2), had an FRP composite tensile failure even though the test unit and loading program were identical to test IV-a (1). The maximum strain in the GFRP composite for test IV-a (1) was 0.55% whereas the maximum measured strain for test IV-a (2) was 1.55%. Fig. 16 shows the small number of fatigue cycles reached in test IV-b.

Due to the varying results obtained to date, the behavior of Series (IV) tests cannot be adequately described. One theory is that the new aluminum pipes do not have as good bonding properties as the field specimens; this might be attributed to oxidation of the field samples. Further testing of reclaimed aluminum pipes from the field will show if this theory is correct.

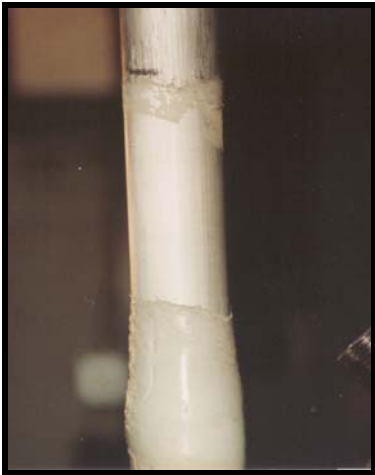


Fig. 15. Adhesive failure of test IV-c

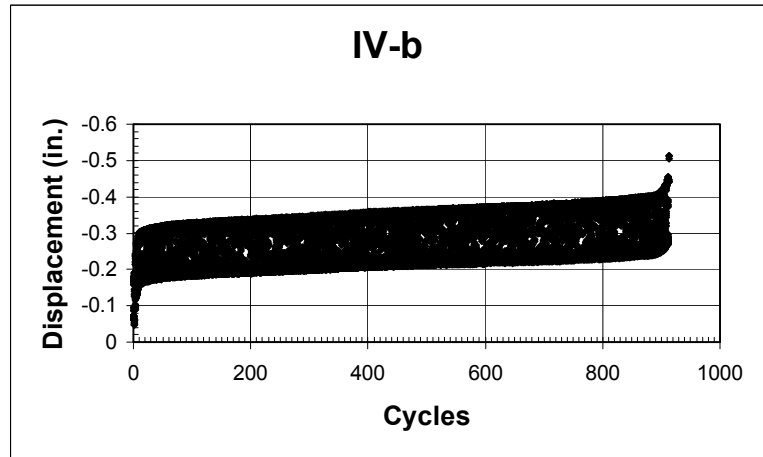


Fig. 16. Displacement vs. Cycles curve for test IV-b

A summary of the experimental results for all four series is given in Table 6. The static tests show a mean ultimate tensile load of 28.6 kips. This value is slightly higher than the one test carried out in the previous investigation (Pantelides and Nadauld 2001). This is due to the better quality of the weld in the present tests.

The results of the three fatigue series are also shown in Table 6. In all three series, three tests were carried out at 21kips, 15kips, and 10kips maximum load. The stress ratio was approximately 0.20 for all tests. In Series (II), for the as-is welded joints, the largest number of cycles experienced was 320,829 cycles. In Series (III), for the repaired joints from the field with GFRP composite, the largest number of cycles experienced was 1,000,000. In Series (IV), for the tack-welded joints with new aluminum pipes and GFRP composite, the largest number of cycles experienced was 27,115.

Fig. 17 shows the S-N curves for all fatigue tests. It can be observed that the as-is welded test units and the repaired joints from the field with GFRP composite show similar behavior. The repaired units from the field with GFRP composite showed better fatigue behavior for the lower stress range. On the other hand, the tack-welded joints with new aluminum pipes and GFRP composite did not perform as well as Series (II) and (III).

Table 6. Summary of Experimental Results

Series I: Test Results for Static Tests of As-is Welded Aluminum Connections with no visible cracks.

Specimen	Type**	Failure	Maximum Load
I-a*	II	Weld & Base	28.81 kips
I-b*	II	Weld & Base	28.26 kips

Series II: Test Results for Fatigue Tests of As-is Welded Aluminum Connections with no visible cracks.

Specimen	Type**	Failure	Maximum Load	R	Number of Cycles
II-a (1)*	I	Weld	21 kips	0.190	5,690
II-a (2)	I	Weld & Base	21 kips	0.190	14,448
II-b (1)*	II	Weld & Base	15 kips	0.267	28,491
II-b (2)	II	Weld & Base	15 kips	0.267	48,096
II-c	II	Weld & Base	10 kips	0.200	320,829

Series III: Test Results for Fatigue Tests of Cracked Aluminum Connections from the field repaired with GRRP.

Specimen	Type**	Failure	Maximum Load	R	Number of Cycles
III-a	II	Weld, Base, & FRP	21 kips	0.19	6,763
III-b	I	Weld, Base, & FRP	15 kips	0.267	69,194
III-c ⁺	II	Infinite Life	10 kips	0.200	1,000,000

⁺After 1,000,000 cycles the static tensile load capacity was = 20.9 kips

Series IV: Test Results for Fatigue Tests of Tack-welded Aluminum Connections Retrofitted with GFRP.

Specimen	Type**	Failure	Maximum Load	R	Number of Cycles
IV-a (1)	I	Adhesive	21 kips	0.19	18
IV-a (2)	I	FRP	21 kips	0.20	30
IV-b	I	FRP	15 kips	0.20	913
IV-c	I	Adhesive	10 kips	0.20	27,115

* = No pipe in the chord

** = Refers to size of the specimen, see Table 5

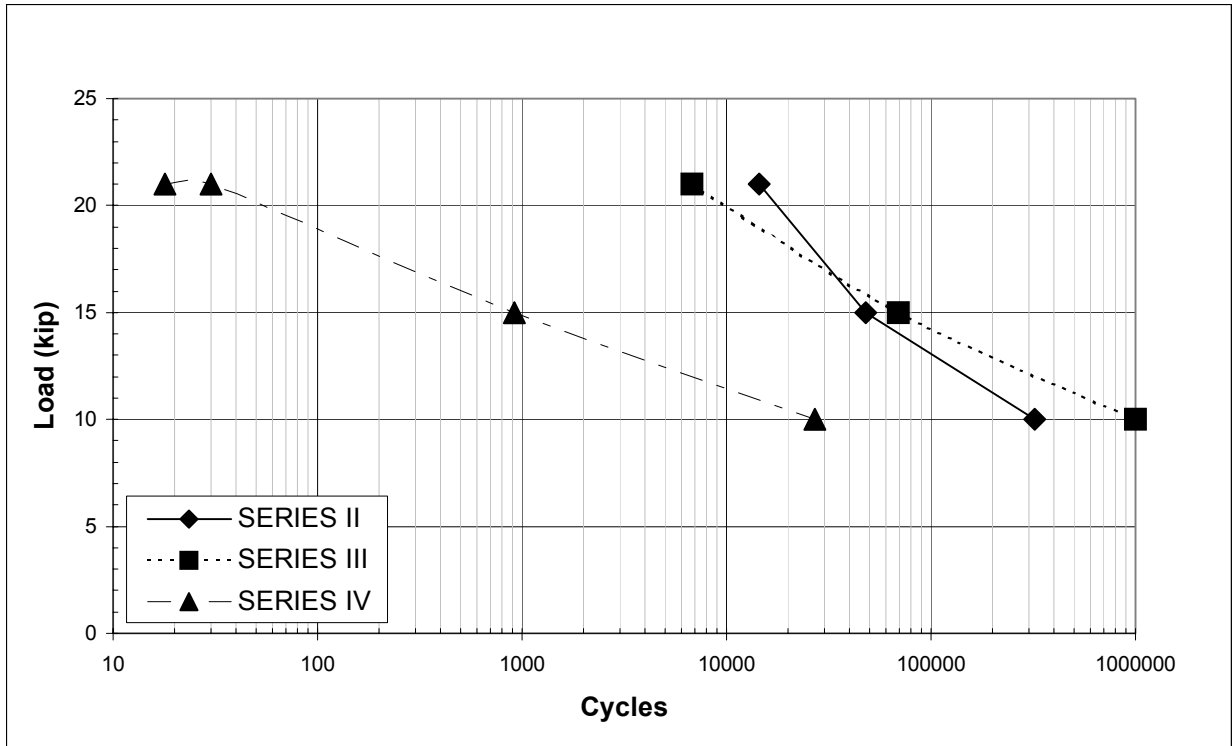


Fig. 17. S-N Curves

5. Preliminary Observations and Conclusions

The static tests, Series (I), performed as expected but with a higher ultimate load than experienced in the previous study by a factor of 1.16; this is attributed to the better quality of the welds in the test units used for the static tests. The failure mode for both static tests was due to a crack initiating at the toe of the weld and continuing almost entirely around the chord.

For the fatigue portion of this study each series exhibited its own failure mode; in some cases more than one failure mode was experienced within the same series. In Series (II), for the as-is welded joints, a single failure mode was experienced. The failure mode started with a crack at the toe of the weld, and then the crack propagated into the base material of the chord.

In Series (III), for the repaired joints from the field with GFRP composite, two distinct failure modes were observed. Failure Mode 1 was due to weld throat cracking and subsequent FRP composite tensile failure. Failure Mode 2 was due to cracking at the toe of the weld followed by cracking of the throat of the weld and subsequent FRP composite tensile failure. Overall, Series (III) performed better than Series (II) especially at the lower stress range.

In Series (IV), for the tack-welded joints with new aluminum pipes and GFRP composite, two distinct failure modes were observed. The first failure mode was an adhesive failure in which the diagonal brace pulled out of the FRP composite at lower strains than ultimate of the FRP composite. The second failure mode was tensile failure of the FRP composite, in which the FRP composite achieved a high percentage of its ultimate strength. Due to the varying results obtained to date, the behavior of Series (IV) tests cannot be adequately described. One theory is that the new aluminum pipes do not have as good bonding properties as the field specimens; this might be attributed to oxidation of the field samples. Further testing of reclaimed aluminum pipes from the field will show if this theory is correct.

Bearing in mind that the test units from the field have already been in service for a number of years, the behavior of Series (II) and Series (III) is satisfactory. This fact also justifies the use of 1,000,000 cycles as the maximum applied number of cycles to indicate infinite life of the joints. The remaining tests, which will be carried out at the lowest stress range, are believed to be necessary to completely describe the likely fatigue stresses experienced by the joints in the field.

6. References

Aluminum Association Inc. (1986) *Aluminum Construction Manual*, Section 1 – Specifications for Aluminum Structures, 5th Ed., Washington, D.C.

American Association of State Highway and Transportation Officials (1975). *Standard Specifications for Structural Supports for Highway Signs, Luminaires and Traffic Signals*. AASHTO Subcommittee on Bridges and Structures, Washington, D.C.

American Association of State Highway and Transportation Officials (1998). *LRFD Bridge Design Specifications, SI Units – Second Edition*, Washington, D.C.

American Association of State Highway and Transportation Officials (2001). *Standard Specifications for Structural Supports for Highway Signs, Luminaires and Traffic Signals*. 4th Edition, Washington, D.C.

Pantelides, C.P., and Nadauld, J. (2001). “Repair of cracked aluminum overhead sign structures with fiber reinforced polymer composites.” *Research Report CVEEN-01/01*, Dept. of Civil & Environmental Engineering, Univ. of Utah, Salt Lake City, Ut.

Sharp, M.L. (1993). *Behavior and Design of Aluminum Structures*. McGraw-Hill, New York, NY.

Sharp, M.L., Nordmark, G.E., and Menzemer, C.G. (1996). *Fatigue Design of Aluminum Components and Structures*. McGraw-Hill, New York, NY.

Steckel, G.L. (2000). “Environmental durability of Hexcel Corporation Hex 3R Wrap 107/Hex 3R Epoxy 300 E-Glass Reinforced Epoxy Composite.” *Tech. Rep. Contract SAMPE 00001*, Air Logistics Corporation, El Segundo, Ca.